

High heat flux testing of plasma facing materials and components – Status and perspectives for ITER related activities

J. Linke ^{a,*}, F. Escourbiac ^d, I.V. Mazul ^b, R. Nygren ^c, M. Rödiger ^a,
J. Schlosser ^d, S. Suzuki ^e

^a *Forschungszentrum Jülich GmbH, EURATOM Association, IEF-2, D-52425 Jülich, Germany*

^b *D.V. Efremov Scientific Research Institute of Electrophysical Apparatus, St. Petersburg 189631, Russia*

^c *Sandia National Laboratories, P.O. Box 5800, Albuquerque, NM 87185, USA*

^d *Commissariat à l'Energie Atomique, CEN Cadarache, F-13108 St. Paul-lez-Durance cedex, France*

^e *Department of Thermonuclear Fusion Research, JAEA, Naka-machi, Ibaraki-ken 311-01, Japan*

Abstract

A broad spectrum of high heat flux test facilities are being used worldwide to investigate the thermal response of plasma facing materials and components to fusion relevant thermal loads. These tests cover both normal operation scenarios with cyclic thermal loads and power densities in the range of several MW m^{-2} and transient heat load tests to simulate short events such as edge localized modes, plasma disruptions and vertical displacement events. There is an urgent need for reliable quality control methods and non-destructive analyses during the procurement phase of ITER; most of these techniques are based on heat flux methods. To quantify irradiation induced property changes and to evaluate the overall performance of neutron irradiated components, miniaturized plasma facing components have been irradiated in fission reactors and post-irradiation tested. Furthermore, in-pile tests have been carried out in order to study the synergetic effects of heat loads and neutron loads.

© 2007 Elsevier B.V. All rights reserved.

1. Introduction

Extensive R&D programmes have been initiated by all ITER partners to develop reliable plasma facing components for the next step fusion experiment [1–3]. These activities focus on the selection and fab-

rication of new, improved plasma facing materials (PFM), primarily based on beryllium for the first wall and on carbon and tungsten for the divertor region [4,5]. Another material related issue is the joining of these PFMs to an effective water cooled heat sink made from copper alloys and/or stainless steel. The joining techniques which have been applied include high temperature brazing, diffusion bonding, HIPping, and electron beam welding. Coatings (CVD, PVD, and 5–10 mm thick coatings

* Corresponding author. Tel.: +49 2461 613230; fax: +49 2461 618312.

E-mail address: j.linke@fz-juelich.de (J. Linke).

applied by plasma spraying) also play an important role, particularly with regard to future repair processes after long term plasma exposure.

Existing fusion devices do not provide the conditions needed to evaluate the performance of PFMs and plasma facing components (PFC) under ITER specific thermal loads, i.e. quasi-stationary heat fluxes up to approximately 10 MW m^{-2} ($\leq 20 \text{ MW m}^{-2}$ during slow transients for a duration of $<10 \text{ s}$) and sufficiently large cycle numbers. Hence, high heat flux test facilities based on intense electron and ion beams have been utilized successfully to assess the efficiency and the fatigue life of different material approaches and design concepts. Modelling and experiments with both normal operation scenarios and transient events, such as plasma instabilities (vertical displacements, plasma disruptions) or edge localized modes (ELMs), are being performed to evaluate and to quantify the resulting material erosion or damage and thus to assess the life-time of the components.

During the procurement phase of the plasma facing components for ITER the development of reliable methods for non-destructive testing (NDT) of industrially manufactured components are gaining significant importance; some of these techniques are based on heat flux methods. Further research activities are focussed on the degradation of materials and joints due to energetic neutrons.

2. High heat flux testing of plasma facing components

To simulate the surface heat flux to plasma facing components a number of different test facilities have been established worldwide [6,7]. To simulate quasi-stationary thermal loads, i.e. thermal loads with pulse durations of at least several seconds to achieve a thermal equilibrium, high heat flux (HHF) test facilities using electron or ion beams are most frequently used. Table 1 shows a selection of the most important test devices which are in operation today. The technology to generate intense focussed electron beams is well established, e.g. in the area of electron beam welding. Hence, the major fraction of the present day electron beam HHF test facilities is based on focussed electron beams with typical diameters of 1–10 mm and particle energies of 30–200 keV. To guarantee a homogeneous heat load distribution in the wall component, a high frequency scanning mode is applied, cf. Fig. 1. Depending on the beam power, the size of the vacuum chamber and the scanning generator, surface areas up to 1 m^2 can be

Table 1
Test facilities for high heat flux testing of plasma facing components

Facility	Particle type	Particle energy (keV)	Beam power (kW)	Max. loaded area (m^2)	Power density (GW m^{-2})	Remarks	Institute partner	
A	TSEFEY	e^-	30	60	0.25	0.2	Scanned beam, $\phi = 20 \text{ mm}$ beryllium	Efiremov RF
B	JUDITH 2	e^-	30–60	200	0.25	10	Scanned beam, $\phi \approx 5 \text{ mm}$ beryllium + irradiated samples	FZJ EU
C	FE 200	e^-	200	200	1.0	60	Scanned beam, $\phi \approx 2\text{--}3 \text{ mm}$ hot coolant loop	CEA EU
D	JEBIS	e^-	100	400	0.18	2	Beam sweeping $\phi \approx 1\text{--}2 \text{ mm}$	JAEA JA
E	EB 1200	e^-	40	1200	0.27	10	Scanned beam, $\phi \approx 2\text{--}12 \text{ mm}$ hot coolant loop	SNLA US
F	PBEF	H^+, He^+	50	1500	0.1	0.06	Two ion sources à 0.75 MW $\phi \approx 150 \text{ mm}$	JAEA JA
G	GLADIS	H^+	50	2200	0.3	0.05	Two ion sources à 1.1 MW $\phi \approx 70 \text{ mm}$	IPP EU

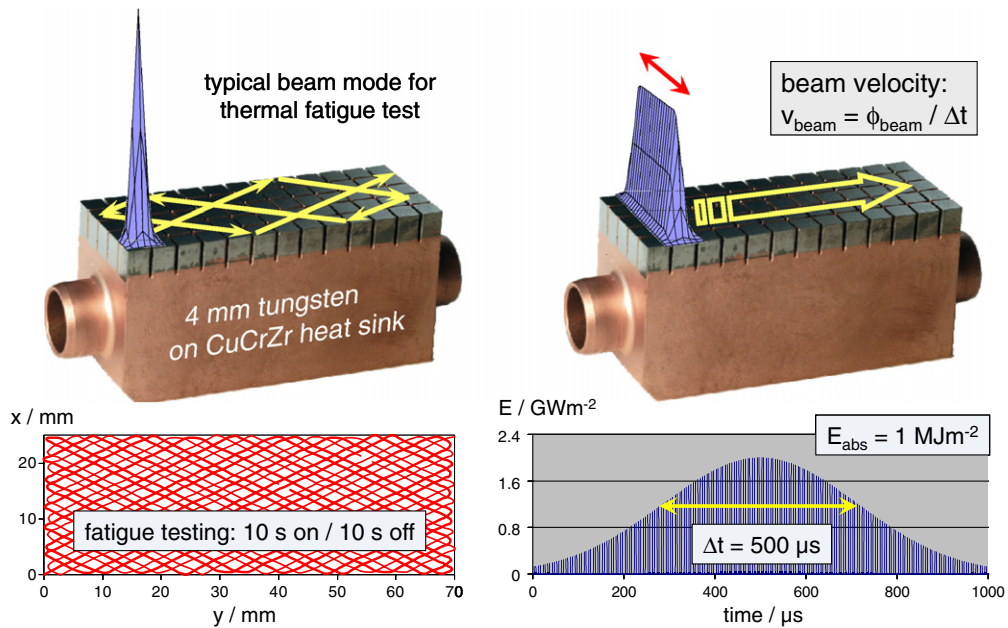


Fig. 1. Electron beam scanning during thermal fatigue tests (left) and transient thermal loads (right).

exposed to uniform thermal loads; test devices with more sophisticated scanning generators can also generate characteristic load patterns, such as peaked profiles to simulate the thermal loads in the divertor strike zone. Other HHF test facilities are based on ion heating; here powerful stationary (i.e. non-scanned) beams of hydrogen or helium ions with diameters of up to several tens of centimetres are utilized to generate fusion specific surface heat fluxes of several tens of MW m^{-2} . It should be noted that electron beams deposit their energy in a thin surface layer (up to approximately $100 \mu\text{m}$ deep in low- Z materials such as carbon or beryllium), and that a fraction of the incident beam energy is reflected due to back-scattered electrons (this fraction may reach values up to 50% for high- Z materials such as tungsten). To simulate surface heat fluxes on typical first wall components (e.g. the primary first wall in ITER with max. thermal loads below 1 MW m^{-2}) infrared test facilities are being used as well. However, due to the limitations in the surface temperatures of the heaters, the resulting heat fluxes are limited to first wall applications; divertor specific thermal loads with power densities of 5 MW m^{-2} and beyond can only be realized in electron and ion beam test devices.

2.1. Thermal fatigue testing

In order to evaluate the thermo-mechanical performance of various divertor designs under cyclic

thermal loads, a large number of small scale divertor and first wall components have been manufactured by industry and research laboratories. These cover different design options (flat tile, saddle type, monoblock) and different joining techniques (high temperature brazing, HIPing, diffusion bonding, electron beam welding) for the applied armour materials (CFC, tungsten and beryllium).

The heat flux limits which have been obtained so far in electron beam experiments (test facility JUDITH, [7]) on small scale mock-ups with typical cycle number of $n = 1000$ can be summarized as follows:

- CFC flat tiles withstood cyclic thermal loads up to $\sim 20 \text{ MW m}^{-2}$ without any sign of failure,
- CFC monoblocks have been tested successfully up to $\sim 25 \text{ MW m}^{-2}$,
- tungsten flat tiles (macrobrush design) did not show any failure up to $\sim 18 \text{ MW m}^{-2}$,
- tungsten monoblocks (drilled W-tiles and W-lamellae) withstood HHF up to $\sim 20 \text{ MW m}^{-2}$.

These test results even exceed the heat flux limits which are expected in next step fusion devices [3]. The data show very clearly that technically mature solutions for the divertor targets are feasible which meet the HHF requirements for ITER during normal operation conditions and during slow transients.

However, the major fraction of the above mentioned heat flux tests have been performed on small scale mock-ups only, i.e. on water cooled components which represent an ITER like cross-section in scale 1:1, but linear extensions of typically less than 1/10 of the components required for ITER. Hence, a number of medium and full scale components for the ITER divertor targets and the baffle component have been manufactured to prove the industrial feasibility and later, to demonstrate their thermal performance under ITER specific thermal loads [8]. The test modules which are representative of the full scale ITER target elements with both, tungsten and CFC armoured sections are shown in Fig. 2. These components have been tested under cyclic thermal loads with up to 3000 cycles in the electron beam test facility FE200 operated by CEA/Framatome. These experiments clearly reconfirm the excellent heat removal efficiency and fatigue resistance of carbon and tungsten armoured components.

Similar to the divertor applications, extensive efforts have been allocated to the development and thermo-mechanical testing of beryllium armoured components for first wall applications [2]. Best performances obtained so far with thermal fatigue tests in electron beam test facilities were heat flux limits up to 11 MW m^{-2} for brazed joints [9]; modules manufactured by hot isostatic pressing have shown detachments of Be tiles after cyclic operation only for heat fluxes $>2.75 \text{ MW m}^{-2}$. These heat fluxes are far above the load limits for the primary first wall in ITER of approximately 0.5 MW m^{-2} .

2.2. Critical heat fluxes

Beside the choice of the materials in plasma facing components, i.e. the plasma facing material and heat sink, the selected joining technique plays also an important role in determining the heat load limits and the resistance against low cycle fatigue. Furthermore, the type of the coolant (water in ITER, He or liquid metal in future fusion devices), the coolant parameters (flow rate, inlet temperature and pressure), and the geometry of the coolant channel play an important role in determining the thermal efficiency of the actively cooled component. In particular for water cooled divertor targets in next step fusion reactors the heat removal limitations due to critical heat fluxes (CHF) have to be thoroughly determined to avoid unanticipated material damage. This phenomenon has been investigated carefully for a number of different coolant channel geometries such as the circular cross-sections with swirl tube inserts, the hypervapotron with coolant fins perpendicular to the coolant flow [10], and a screw-type coolant channel [11]. At high flow rates CTF values of 40 MW m^{-2} and beyond have been achieved; these data provide satisfactory safety margins against burn-out failure.

2.3. Thermal shock testing under short transient loads

The plasma facing components in ITER will also be subjected to a number of short transient events with extremely high energy densities [12]. These



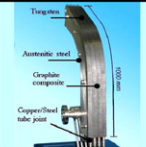

Mock-ups				
Name of Mock-up	VTMS	VTMSDEF	VTFS	BAFFLE
Year of tests	1998-1999		2004	2004
CFC part material	NB31	NB31	NB31	NB31
Top CFC thickness	13.5 and 7.5 mm	13.5 mm	5 mm	4 mm
Monoblock width	23 mm	23 mm	23 mm	23 mm
CFC/Cu Joint	AMC	AMC	AMC	AMC
Cu-Tube joint	Brazing	Brazing	HIPing	HIPing
Nb of cycles	$1000 \times 10 \text{ MW/m}^2$	$1000 \times 12 \text{ MW/m}^2$	$1000 \times 10 \text{ MW/m}^2$	$3000 \times 10 \text{ MW/m}^2$
	$2000 \times 20 \text{ MW/m}^2$	No propagation of cal. defects	$1000 \times 20 \text{ MW/m}^2$ $1000 \times 23 \text{ MW/m}^2$	$500 \times 16 \text{ MW/m}^2$
W part material	W	W	WL10	
Geometry	macrobrush	macrobrush	monoblock	
W thickness	10 mm	10 mm	5 mm	
Monoblock width	23 mm	23 mm	23 mm	
Nb of cycles	$1000 \times 10 \text{ MW/m}^2$	$1000 \times 10 \text{ MW/m}^2$	$1000 \times 15 \text{ MW/m}^2$	
	$1000 \times 15 \text{ MW/m}^2$		$1000 \times 20 \text{ MW/m}^2$	

Fig. 2. High heat flux testing of medium and full scale components for the ITER divertor and the baffle, electron beam test facility FE-200.

incidents are partially off-normal events, i.e. plasma disruptions with energy densities of a few up to several tens of MJ m^{-2} and plasma instabilities, so-called VDEs (vertical displacement events) with energy densities of $\leq 60 \text{ MJ m}^{-2}$. The energy deposition during disruptions is in the millisecond range, while the VDEs occur on a much longer timescale ($\Delta t \approx 100\text{--}300 \text{ ms}$). In ITER both events can result in substantial material erosion due to melting and/or evaporation processes. Hence, the number of these life-time limiting events has to be kept within specified limits (less than 10% and 1% of all plasma discharges should be terminated by such an incident, respectively).

Carbon based materials, in particular carbon fibre composites (CFC) with multidirectional fibre orientation and high thermal conductivity values (perpendicular to the plasma facing surface) turned out to be more forgiving than refractory metals due to the absence of any solid–liquid phase transition. Therefore, the x -point strike zone on the divertor targets will be made from this material. However, the thermal erosion under intense transient loads may increase significantly due to brittle destruction processes [13]. This effect has been observed experimentally in HHF test facilities and has been benchmarked by numerical methods [14]. The hot particles which were emitted from the electron beam exposed surface have been collected and identified as fibre fragments and clusters of fibres with a maximum size of $100 \mu\text{m}$. Below a threshold value (at approximately 2.5 GW m^{-2} for pulse durations of 2 ms) the brittle destruction process is terminated abruptly. The surface analysis of the 3-directional CFC NB31 by SEM methods shows a clear erosion of PAN fibres (Fig. 3) which are oriented parallel to the surface of the test sample – the pitch fibre bundles, which are oriented perpendicular to the plasma facing surface, remain almost unaffected. The same process has also been observed for isotropic fine grain graphite; here the threshold values is slightly shifted towards lower energy densities, and the collected particles consist of graphitic grains and grain clusters. When approaching the threshold value, the eroded particles consist mainly of tiny dust particles originating from the binder phase. In any case, the erosion products (fibre fragments or graphite grains) are emitted at a relatively high speed (up to 150 m s^{-1}) and thus represent a major source for the generation of carbon dust particles.

The response of metals to intense transient thermal loads is strongly affected by the energy density

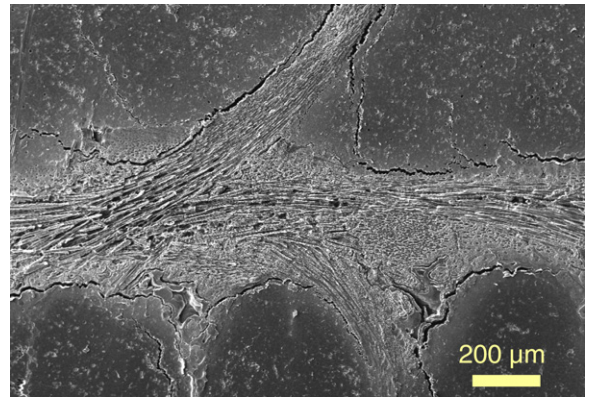


Fig. 3. Disruption simulation test on the carbon fibre composite NB31 ($\Delta t = 5 \text{ ms}$, $P_{\text{abs}} = 2320 \text{ MW m}^{-2}$).

of the incident beam pulse. For low energy densities below the melting threshold the formation of micro-cracks and/or roughening of the sample surface has been observed under repeated pulses. Above the melting threshold, the liquefied material will either remain in the position where it is formed and recrystallize after a short period, or it will be ejected due to the high vapour pressure at the surface of the melt pool. A further increase of the incident power density may also initiate boiling processes and droplet formation of the melt layer. These processes are a major source for the formation of metallic droplets, particularly if additional (e.g. magnetic) forces are acting on the melt layer. These droplets (typical velocities in the order of 10 m s^{-1}) might contaminate the plasma. The recrystallized melt layer forms a dense crack pattern with a crack orientation preferentially perpendicular to the melt layer surface. Deep cracks have also been observed in the sample surface in areas which have not been exposed to the incident beam; here high stresses induced by steep thermal gradients are obviously the driving force for this type of material response [15]. It also should be noted that the formation of (inter-granular) cracks in tungsten can be significantly suppressed if the temperature of the test samples is kept above the ductile–brittle–transient–temperature (DBTT).

A number of powerful test facilities are also available to evaluate the material degradation under short transient events. The motivation to utilize these complex test facilities for fusion materials research are two-fold. First of all, the material response to very short events, namely to type I ELMs which are expected in ITER to occur at a frequency of about 1 Hz is almost unexplored. On the other hand, the wall materials in inertial fusion

energy (IFE) experiments will be subjected to even shorter pulses with higher power density values and higher repetition rates. Fig. 4 shows these loading parameters for short transient incidents in inertial confinement and in magnetic confinement conditions. To allow for a better comparison of the applied damage levels, the y-axis shows the heat flux parameter, which is the product of power density and the square root of the pulse duration – the x-axis is the duration of the events. Typical pulses in laser fusion devices are in the order of 3 μ s; ELMs in ITER will occur in a time frame of 100–500 μ s. The heat flux parameter $P \cdot t^{0.5}$ is in the same order of magnitude for both events these data have to remain below the melting threshold if tungsten is used as a wall material. Additional circles in this diagram represent the ITER specific loading conditions for disruptions, VDEs and normal operation conditions for the divertor. Furthermore, the plot displays data points for transient load tests on tungsten samples in a number of different test facilities, namely the electron beam facility JUDITH, the quasi-stationary plasma accelerator QSPA Kh-50 in Kharkov, Ukraine, the plasma gun MK200-U in Troitsk, Russia, and the Repetitive High Energy Pulsed Power ion source RHEPP-1 in Albuquerque, USA. These tests cover a rather wide range of different pulse durations, nevertheless, the observed

threshold values for the above mentioned damage factors (R = roughening, C = cracking, M = melting, B = boiling) appear at similar heat flux parameters $P \cdot t^{0.5}$. It should be noted that this plot contains only preliminary results which have been obtained from different test specimens (i.e. tungsten with different grain size and orientation etc.). Nevertheless, this first attempt to compare data from a number of very different test facilities using electron, plasma or ion heating might be a basis for a combined effort to tackle the material issues under very short thermal exposure.

Up to now the simulation of sub-millisecond events (ELMs, IFE) has been performed with only relatively low cycle numbers; large pulse numbers (e.g. $>10^6$ ELM pulses during the life-time of the ITER divertor) are not feasible in the majority of the above mentioned test facilities. Most of these ion or plasma accelerators have repetition rates in the order of several minutes or longer which makes the simulation ITER or IFE relevant pulse numbers almost impossible. Here electron beam test facilities are more flexible; this applies in particular to the latest generation of e-beam devices with very fast and flexible beam control units. Fig. 1 compares the beam mode in standard thermal fatigue tests (left) with the so-called ‘ELM-mode’ (right). Thermal fatigue testing requires a rather uniform heat

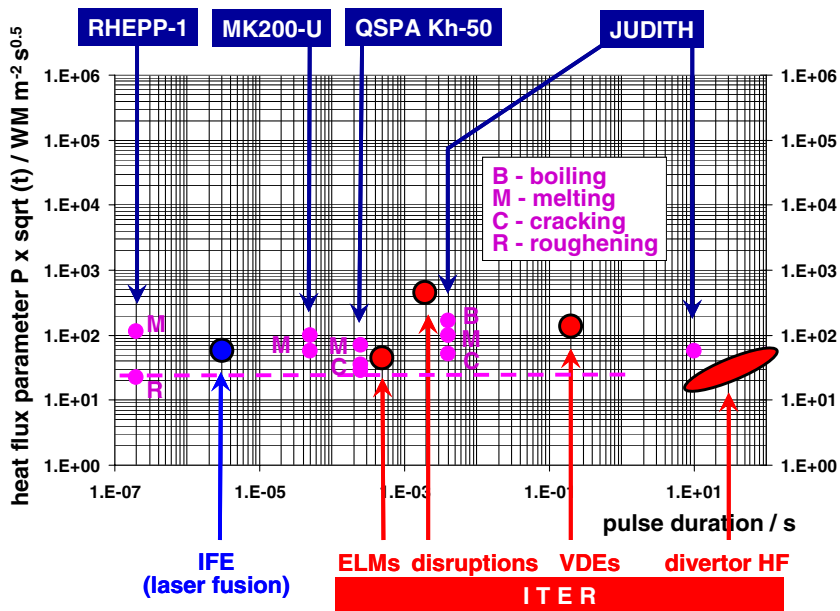


Fig. 4. Simulation of short transient events with tungsten test specimens in a number of different electron, plasma and ion beam test facilities.

load distribution on the full sample surface; this is established by a focussed beam which is scanned across the full surface of the actively cooled component. Typical surface heat loads in this mode are from $\approx 1\text{--}20\text{ MW m}^{-2}$ with fatigue cycles of typically 20 s. This mode has also been used to simulate VDEs or plasma disruptions; however, to achieve the necessary surface power densities of several hundred MW m^{-2} or beyond, the scanned area has to be limited to approximately 1 cm^2 for VDEs and only a few tens of mm^2 for disruptions, respectively.

In principle this process can also be applied to simulate edge localized modes (type I ELMs); this requires a well focussed beam with peak power densities well above 2 GW m^{-2} and a fast beam control unit. Nevertheless, the heat affected area is only a few mm^2 and lateral losses due to heat conduction might complicate a precise wall loading. Therefore another beam mode has been selected to generate repeated ELM-specific pulses with a high repetition rate, cf. Fig. 1. To generate a relatively wide heat flux footprint, the electron beam is scanned parallel to the axis of the components with the highest available frequency. This elongated electron beam pattern is then moved across the full specimen surface; to guarantee a thermal pulse with ELM specific parameters the velocity of the beam motion parallel to the coolant tube must be as follows: $v_{\text{beam}} = \phi_{\text{beam}}/\Delta t$.

To generate high cycle numbers, the ‘ELM-mode’ has to be repeated periodically. This can be done either in a mode which simulates a typical ITER pulse, i.e. a fast scanning mode to simulate the normal operation heat flux of $\approx 5\text{ MW m}^{-2}$ and once per second a fast switch to the ‘ELM-mode’ (Fig. 5). This mode allows the simulation of

approximately 20000 ELM events per working day. In an accelerated mode, which operates without the triangular beam scanning, ELM events can be simulated with a frequency of 5 Hz (i.e. ≈ 100000 events per working day).

3. Heat flux tests for non-destructive investigation

To guarantee the safe operation of this HHF component under normal and off-normal events, a careful inspection of all plasma facing components during the procurement phase is indispensable [1,16]. This challenging task can only be established by highly reliable non-destructive testing procedures. In particular during the first stage of the manufacturing process, i.e. the joining of the PFC-tiles to the heat sink, ultrasonic inspection and X-ray techniques will be utilized. However, after the assembly of the individual target elements the access to these techniques is limited and heat flux methods are mandatory.

Therefore high heat flux testing of full wall components in large electron or ion beam test facilities will be performed to provide evidence that the mock-up is free from any defect in the armour – heat sink joint. According to the ITER procurement plan the first 10% of all industrially manufactured divertor components will be subjected to a meticulous HHF testing; 10% of the remaining components have to be tested in a similar way. Beside electron beam testing, an equivalent diagnostic tool, namely non-destructive testing by infrared methods has been developed and is now fully operational [17,18]. This method is based on a careful diagnosis of the temperature distribution of the plasma facing surface under coinstantaneous streams of cold and hot water in the coolant tubes. Any defect in the joining interface can be clearly detected by a sensitive IR camera from a delayed temperature adjustment of defective armour tiles. Selecting a $\Delta T_{\text{ref}} = 3\text{ K}$ as an acceptance criterion, allows to detect defects with a size down to approximately 4 mm. Fig. 6 shows experimental evidence that infrared test in the SATIR facility and electron beam tests (FE200) provide comparable results.

4. Irradiation induced degradation of plasma facing components

Compared to thermonuclear fusion reactors generating electrical power (DEMO and beyond), the

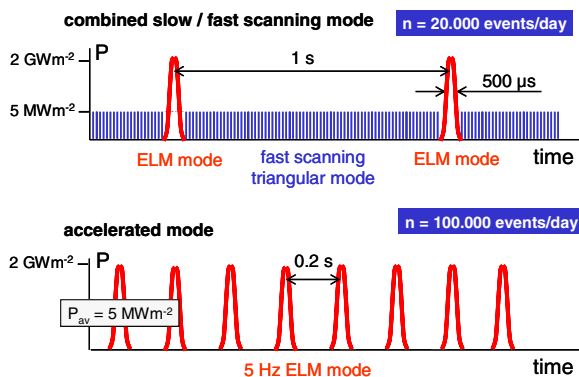


Fig. 5. Electron beam simulation of ELMs with high cycle numbers top: combined thermal fatigue and ELM loads bottom: accelerated mode (sample heating by ELM loads only).

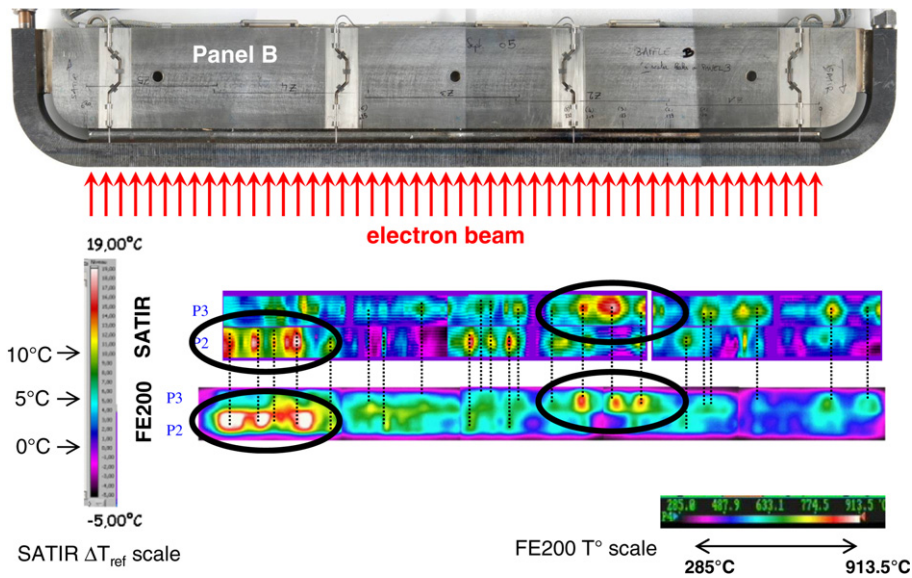


Fig. 6. Electron beam testing (FE200) and infrared inspection (SATIR test) on a baffle mock-up for ITER.

next step ITER device is characterized by significantly lower neutron fluences to the plasma facing components. Here the integrated fluence will remain below 1 dpa for the plasma facing material and below 3 dpa for the Cu alloys in the heat sink for the ITER divertor. To investigate the neutron induced degradation of plasma facing components, test specimens from all relevant materials have been irradiated in material test reactors to ITER specific neutron doses. On these samples a number of thermo-physical and thermo-mechanical parameters have been determined [19]. Electron beam high heat flux tests have also been applied to un-irradiated and neutron irradiated divertor components to evaluate the neutron effect on the heat removal efficiency and the fatigue performance of these mock-ups.

The results which have been obtained so far at an irradiation temperature of 200 °C can be summarized as follows [20]:

- CFC flat tiles have been exposed to cyclic thermal loads up to 15 MW m^{-2} (at 0.2 dpa and 1.0 dpa in C) and for 1000 thermal cycles without any failure,
- CFC monoblocks have been tested up to 12 MW m^{-2} for 1000 cycles,
- tungsten monoblock modules did not show any failure up to 18 W m^{-2} (0.1 and 0.6 dpa in W),
- tungsten flat tiles (macrobrush) withstood 1000 cycles at 10 MW m^{-2} (0.1 and 0.6 dpa); the fati-

gue tests were characterized by a significant increase of the surface temperature.

Compared to tungsten, the thermal conductivity of CFC decreases markedly; at a fluence of 1 dpa the room-temperature thermal conductivity is only one tenth of the un-irradiated value. The limited power densities for the above mentioned fatigue tests on CFC modules were not due to a failure of the mock-up itself but due to heavy erosion, caused by sublimation of carbon as a result of too high surface temperatures.

Neutron irradiation experiments with beryllium armoured primary first wall mock-ups (low temperature irradiation, 0.6 dpa in Be) are under way.

A major drawback of these post-irradiation experiments is that the irradiation in a material test reactor and the high heat flux testing are performed separately, i.e. recovery processes due to the annealing of the plasma facing material can not occur during the irradiation phase. Therefore, experiments with simultaneous irradiation [21] and high heat flux exposure have been performed in the SM experimental reactor in Dimitrovgrad, Russia. In this test campaign the irradiation capsule was equipped with two actively cooled divertor mock-ups and a nuclear heater to provide divertor relevant heat fluxes during the neutron irradiation phase. This heater consists of tungsten blocks which are in direct thermal contact with the surface of the mock-ups, separated only by a thin layer of soft carbon. The neutron flux

in the core position was $4.9 \times 10^{18} \text{ n m}^{-2} \text{ s}^{-1}$; the surface heat flux in this configuration was $\approx 7 \text{ MW m}^{-2}$. During the in-pile experiment two divertor components with CFC armour (1 CFC flat tile and 1 monoblock module) were actively cooled by the coolant water of the nuclear reactor ($T = 70 \text{ }^\circ\text{C}$, $p = 5 \text{ MPa}$). Cyclic neutron irradiation and thermal loads have been applied by moving the irradiation rig periodically from the core position to the plenum above the core and back; typical dwell times were 600 s in-pile and 60 s out of pile. An effective duration of 188 h was necessary to achieve 1000 cycles; the accumulated neutron fluence was $3.1 \times 10^{20} \text{ n m}^{-2}$ corresponding to approximately 0.3 dpa. Post-irradiation examination of the two components did not show any appreciable deterioration.

5. Conclusions

High heat flux experiments are an important tool for the development of plasma facing components for thermonuclear fusion devices. A number of powerful test beds based on electron and ion beams are available to apply cyclic thermal loads up to $\sim 20 \text{ MW m}^{-2}$; these devices play an important role for the qualification of small, medium and full scale mock-ups, in particular of joints between heat sink and armour material. In addition HHF tests have been used for the evaluation of new coolant concepts (hypervapotron, screw tube) and for the evaluation of their heat removal limitations.

During the industrial manufacturing of plasma facing components for next step fusion experiment such as ITER, reliable non-destructive test methods for component inspection are indispensable. For this purpose, in addition to electron and ion beam HHF testing of full components, infrared diagnostics have also been developed; both methods will be the major NDT-techniques for divertor components in the procurement phase of ITER.

Simulation experiments of short transient events such as vertical displacement events, plasma disruptions, ELMs or even shorter energetic pulses in inertial fusion confinement experiments require powerful test devices capable to generate short pulses with extreme power densities in the GW m^{-2} range. Here in addition to electron and ion beam devices, plasma accelerators represent the most appropriate test beds. Heat load experiments which have been performed on a number of carbon based

or metallic wall candidates show irreversible damage due to melting, crack formation, roughening and brittle destruction. These processes may also be associated with the generation of (carbon, beryllium or tungsten) dust particles.

Neutron irradiation experiments with doses up to 1 dpa clearly affect the heat flux performance of divertor components. In particular CFC armoured modules show a reduced heat removal efficiency due to the strong degradation of the thermal conductivity. Monoblock mock-ups with tungsten armour are by far less susceptible to this degradation effect.

Acknowledgement

Part of this work was carried out within the framework of the European Fusion Development Agreement. The views and opinions expressed herein do not necessarily reflect those of the European Commission or those of the ITER project.

References

- [1] M. Merola, J. Palmer, in: Proc. Intern. Symposium on Fusion Nuclear Technology, Tokyo, 22–27 May, 2005.
- [2] P. Lorenzetto, B. Boireau, C. Boudot, P. Bucci, A. Furmanek, K. Ioki, J. Liimatainen, A. Peacock, P. Sherlock, S. Tähtinen, *Fus. Eng. Des.* 75–79 (2005) 291.
- [3] R. Tivey et al., *Fus. Eng. Des.* 46 (1999) 207.
- [4] H. Bolt, V. Barabash, W. Krauss, J. Linke, R. Neu, S. Suzuki, N. Yoshida, *J. Nucl. Mater.* 329–333 (2004) 66.
- [5] J. Linke, P. Lorenzetto, P. Majerus, M. Merola, D. Pitzer, M. Rödiger, in: Proc. ANS 16th Topical Meeting on the Technology of Fusion Energy, Madison, Wisconsin, 14–16 September, 2004.
- [6] I. Smid, *Mater. Sci. Forum* 475–479 (2005) 1355.
- [7] T. Hirai, K. Ezato, P. Majerus, *Mater. Trans.* 46 (3) (2005) 412.
- [8] M. Missirlian, F. Escourbiac, M. Merola, A. Durocher, I. Bobin-Vastra, B. Schedler, et al., *J. Nucl. Mater.*, these Proceedings.
- [9] A. Gervash, R. Giniyatulin, I. Mazul, R. Watson, in: Proc. 20th Symp. on Fusion Technology, 1998, p. 47.
- [10] J. Schlosser, F. Escourbiac, M. Merola, B. Schedler, P. Bayetti, M. Missirlian, R. Mitteau, I. Bobin vastra, *Phys. Scr.* T111 (2004) 199.
- [11] K. Ezato et al., *J. Nucl. Mater* 329–333 (1) (2004) 820.
- [12] G. Federici et al., *J. Nucl. Mater* 313–316 (2003) 11.
- [13] J. Linke, S. Amouroux, E. Berthe, Y. Koza, W. Kühnlein, M. Rödiger, *Fus. Eng. Des.* 66–68 (2003) 395.
- [14] S.E. Pestchanyi, H. Wuerz, I.S. Landman, *Plasma Phys. Control. Fus.* 44 (2002) 845.
- [15] A. Zhitlukhin et al., *J. Nucl. Mater* 337–339 (2005) 684.
- [16] F. Escourbiac, Ph. Chappuis, J. Schlosser, M. Merola, I. Vastra, M. Febvre, *Fus. Eng. Des.* 56&57 (2001) 285.

- [17] F. Escourbiac, S. Constans, X. Courtois, A. Durocher, V. Casalegno, *J. Nucl. Mater.*, these Proceedings.
- [18] F. Escourbiac, A. Durocher, V. Casalegno, S. Constans et al., *J. Nucl. Mater.*, these Proceedings.
- [19] V. Barabash, G. Federici, J. Linke, C.H. Wu, *J. Nucl. Mater.* 313–316 (2003) 42.
- [20] M. Roedig, W. Kuehnlein, J. Linke, D. Pitzer, M. Merola, E. Rigal, B. Schedler, E. Visca, *J. Nucl. Mater.* 329–333 (2004) 766.
- [21] N. Litunovsky, A. Gervash, V. Komarov, P. Lorenzetto, I. Mazul, R. Melder, *J. Nucl. Mater.*, these Proceedings.